CHEST IMAGING

Iran J Radiol. 2022 July; 19(3):e127182. https://doi.org/10.5812/iranjradiol-127182.

Published online 2022 October 25. **Research Article**

Correlation Between CD4 Cell Count, HIV Viral Load, and Chest CT Findings of AIDS-associated Pulmonary Cryptococcosis

Zixin Zhang [1], Chunshuang Guan [1], Budong Chen [1] and Ruming Xie [1, *]

[1] Beijing Ditan Hospital, Capital Medical University, Beijing, China

[*] *Corresponding author*: Beijing Ditan Hospital, Capital Medical University, Beijing, China. Email: aaxieruming@126.com

Received 2022 April 24; **Revised** 2022 September 19; **Accepted** 2022 September 26.

Abstract

Background: The computed tomography (CT) features of acquired immune deficiency syndrome (AIDS)-associated pulmonary cryptococcosis (PC) are correlated with the viral load of human immunodeficiency virus (HIV). An increase in CD4-positive T lymphocyte (CD4) cell count in peripheral blood after a highly active antiretroviral therapy (HAART) can reflect the morphological changes of lung lesions.

Objectives: This study aimed to evaluate the correlation between CT features and HIV viral load and to determine a cut-off value for CD4 cell count increment to investigate the prognosis of PC. It also aimed to examine the morphology of PC lesions and their prognosis following HAART.

Patients and Methods: Sixty-two patients with AIDS-associated PC, confirmed by pathology or follow-up, were enrolled in this study. The CT findings were recorded and classified as nodular, cavitary, and consolidation groups and their subtypes. Forty HIV patients who had undergone HAART were screened in this study, and the outcomes of lung lesions were recorded in a follow-up of 3 - 6 months. The participants were divided into improvement and progression groups. The correlation analysis and the receiver operator characteristic (ROC) curve analysis were used to examine the correlation between CT morphology and HIV viral load and to determine the cut-off value for CD4 cell count increment. The intraclass correlation coefficient (ICC) for inter-observer agreement was also calculated.

Results: In the nodular group, patients with miliary nodules had the highest HIV viral load in peripheral blood (miliary nodules vs. solitary nodules, P = 0.009; miliary nodules vs. multiple nodules; P = 0.024). In the cavitary group, thick-walled cavity lesions had a higher HIV viral load than thin-walled cavity lesions (thin-walled vs. thick-walled cavity lesions, P = 0.036). Changes in the morphology of lesions, indicating the progression or improvement of PC, had a positive correlation with the CD4 cell count increment (F = 4.260, P = 0.045). The cut-off value for CD4 cell count increment to differentiate the two outcomes (progression and improvement) was 44/μL. The area under the curve (AUC) was 0.851, and sensitivity, specificity, and accuracy were estimated at 0.815, 0.714, and 0.764, respectively.

Conclusion: In AIDS-associated PC, different types of lesions were related to the HIV viral load, and CD4 cell count increment following HAART was associated with the morphological changes of lesions. This finding can be helpful for clinicians and radiologists to make an accurate diagnosis and evaluate the treatment outcomes, as well as disease progression.

Keywords: Pulmonary cryptococcosis, CT, HIV Viral Load, CD4 Cell Count

1. Background

Cryptococcal pneumonia is an opportunistic infection, with the second highest incidence following *Aspergillus* infection in the lungs of patients with human immunodeficiency virus (HIV). It is classified as an invasive pulmonary fungal infection (IPFI), which can easily invade HIV-infected patients in advanced stages of acquired immune deficiency syndrome (AIDS). The CD4-positive T lymphocyte cell count and HIV viral load are known to directly reflect the immune status and serve as indicators in evaluating the progression of AIDS. Besides, they are recognized as important parameters to monitor the occurrence of opportunistic infections and morbidities of patients (1-3).

According to available evidence on pulmonary cryptococcosis (PC) in AIDS patients, cavity within nodules/masses and solitary nodules are the most frequent computed tomography (CT) findings (4, 5). However, no further investigation has explored the relationship between HIV viral load and lesion morphology. Similarly, the correlation between the CD4 cell count increment and the morphological prognosis of lung lesions has been even

Copyright © 2022, Author(s). This is an open-access article distributed under the terms of the Creative Commons Attribution-NonCommercial 4.0 International License (http://creativecommons.org/licenses/by-nc/4.0/) which permits copy and redistribute the material just in noncommercial usages, provided the original work is properly cited.

more rarely studied.

2. Objectives

This preliminary study aimed to investigate the correlation between CT features and HIV viral load and to determine a cut-off value for CD4 cell count increment in differentiating PC prognosis to assist clinicians and radiologists in diagnosis and evaluation of treatment outcomes and disease progression.

3. Patients and Methods

3.1. Patients

This retrospective, single-center study was approved by the Ethics Review Committee of the institution (Beijing Ditan Hospital, Capital Medical University). The following data were collected from the patients' medical records available in Beijing Ditan Hospital between June 2017 and June 2021: Age, sex, clinical features, antiretroviral therapy, CD4 cell count, CD8-positive T lymphocyte (CD8) cell count, HIV viral load, chest CT scan findings, and treatment outcomes. Overall, 62 HIV-infected patients were diagnosed with PC. Forty cases had complete clinical and CT data in the three- to six-month follow-up after highly active antiretroviral therapy (HAART). Flow cytometry (BD Corp., USA) was performed to measure the CD4 and CD8 cell count, and a quantitative fluorescent nucleic acid detection reagent (Millipore Corp., USA) was used to measure the HIV viral load in the patients' peripheral blood.

3.2. Diagnostic Criteria for Cryptococcosis

Definite diagnosis: (1) Positive histopathology, based on the open lung biopsy, percutaneous lung biopsy, and transbronchial biopsy; and (2) positive Cryptococcus culture from the cerebrospinal fluid (CSF) or blood samples.

Possible diagnosis: (1) Positive cryptococcal capsular polysaccharide antigen (CrAg) test in the CSF or serum; (2) typical clinical manifestations (e.g., cough, fever, and expectoration) without other pathogenic bacterial infections; and (3) improvement of patient's condition and/or pulmonary lesions with anticryptococcal therapy alone. A possible diagnosis could be made when both the first and second criteria or both the first and third criteria were met (6, 7).

3.3. Inclusion and Exclusion Criteria

The inclusion criteria were as follows: (1) HIV positivity; (2) presence of a lesion in the lungs; (3) age above 18 years; and (4) a definite or possible diagnosis of PC. On the other hand, the exclusion criteria were as follows: (1) other concomitant underlying diseases compromising immunity; (2) unclear CT scan findings or not meeting the diagnostic requirements; and (3) non-standard HAART.

3.4. Definitions and Interpretations

The lung lesions were classified into three patterns: Solid nodules (S), cavitary nodules (CA), and consolidation (C), based on the number and morphology of lesions. Nodular lesions were further subdivided into solitary nodules (SNs), multiple nodules (MNs with < 5 nodules), and miliary nodules (MINs with countless small and randomly distributed nodules). Besides, cavitary lesions were further subdivided into four types, according to the shape and thickness of the hollow wall: Thick-walled cavity (TKC with a cave wall thickness of 4 - 8 mm) (Figure 1); thin-walled cavity (TNC with a cave wall < 3 mm) (Figure 2A); tiny cavity (TC, cavity area < 20% in a nodule-based component) (Figure 2A-C); and cavity in the wall (CW with multiple tiny holes in the cyst wall from partition to partition) (Figure 2A) (8, 9). Consolidation usually manifested with ill-defined margins to normal lung tissue (Figure 2B).

After the onset of HAART, the morphological changes of lung lesions were classified into two categories: Improvement group and progression group. The improvement group included patients in whom the nodules decreased, or the cavities became nodules, or the cavity walls became thinner. On the other hand, the progression group consisted of patients in whom nodules were enlarged and/or increased, or nodules transformed into cavities, or cavity walls became thicker, or ill-defined margin infiltrations were detected. At least one of these conditions suffices to classify a patient in the corresponding group. Two radiologists with more than 10 years of experience in the diagnosis of infectious diseases, who were blind to laboratory indicators, decided about the morphological classification of lesions and progression according to CT findings, including the location, borders, density, and number of lung lesions, as well as pleural effusion and mediastinal lymph nodes.

3.5. Data Analysis

The collected data were analyzed in SPSS Version 25.0 (IBM Corp. Released 2017. IBM SPSS Statistics for Windows, Version 25.0. Armonk, NY: IBM Corp.). The clinical indicators are expressed as median and interquartile range (IQR), as well as mean ± standard deviation (SD). The normal distribution of data was examined before statistical tests. All data were analyzed in each group using repeated measures multivariate analysis of variance after Mauchly's test of sphericity. Moreover, Bonferroni correction test was used for comparison of the three groups. Moreover, a receiver operating characteristic (ROC) curve was plotted to

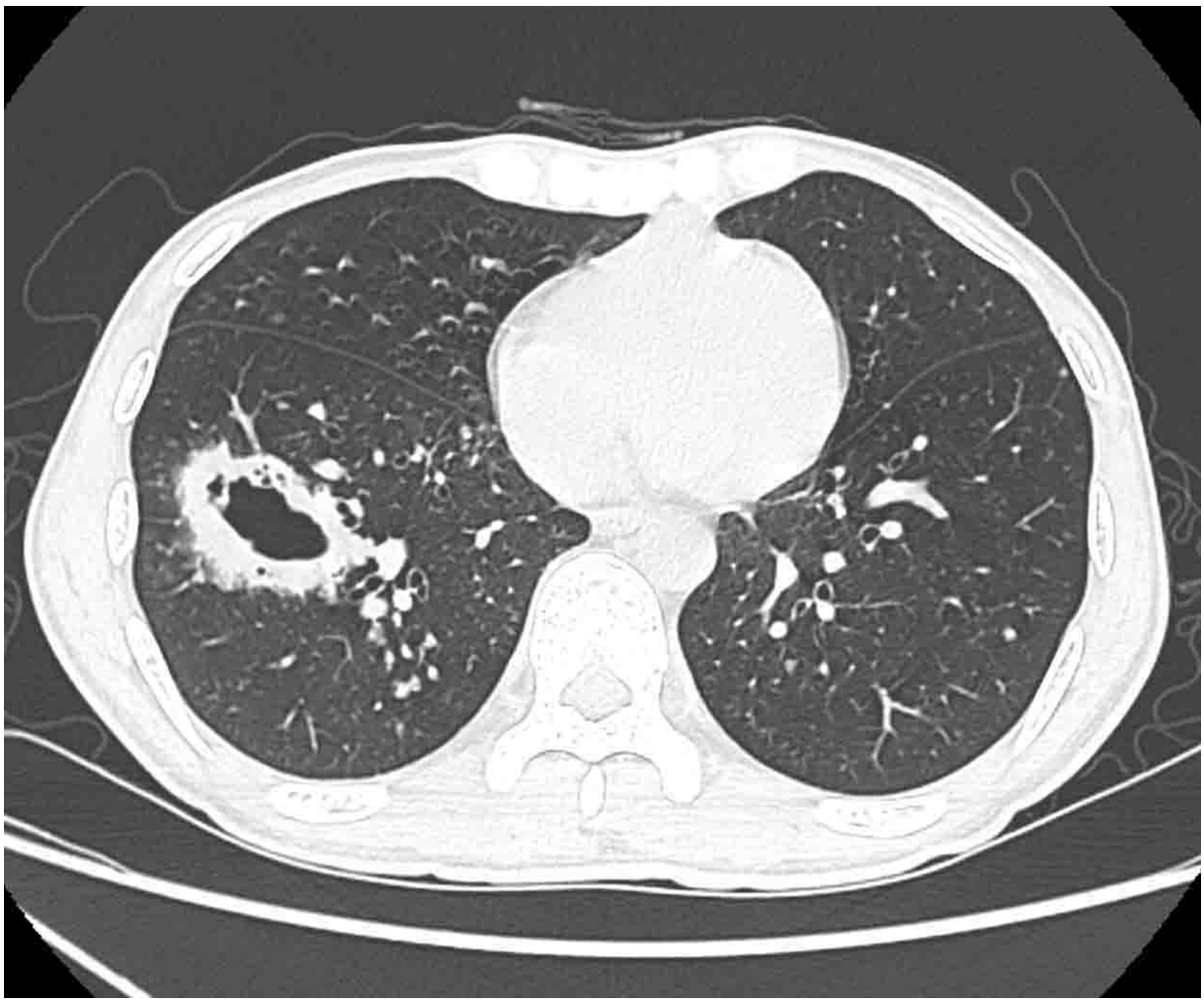

Figure 1. A 27-year-old HIV-infected man with pulmonary cryptococcosis (PC) and a representative thick-walled cavity lesion confirmed by pathology. In the right lower lobe, lesion with irregular thick-walled and line-shaped shadows had an unclear border with the normal lung, while small nodules with sharp borders mixed with ground-glass opacity around the cavity are detected.

evaluate the performance of diagnostic tests and measure the sensitivity, specificity, accuracy, 95% confidence interval (CI), Youden's index, and cut-off value for CD4 cell count increment. The inter-observer agreement for the two radiologists was calculated using the intraclass correlation coefficient (ICC). A P-value less than 0.05 was considered statistically significant, and an ICC >0.8 indicated good agreement.

4. Results

4.1. Basic Clinical Characteristics and Radiological Features of the Patients

The clinical characteristics of the patients are presented in Table 1. Of 62 patients, 18 were included in this study with a definite diagnosis, including six patients with a percutaneous lung biopsy, nine patients with a positive Cryptococcus culture from blood samples, and three patients with positive CSF culture; the remaining patients were included with a possible diagnosis. Overall, 59 (95.2%) patients were male, while 3 (4.8%) patients were female, with a median ages of 36.97 ± 11.91 years (range, 19 - 77 years).

Twenty-three out of 62 patients presented to the hospital with multiple symptoms. The main clinical symptoms of 19 patients were pulmonary symptoms; 32 patients first developed neurological symptoms; and 39 patients had fever or fever combined with other symptoms. All cases were complicated with pulmonary complications or other

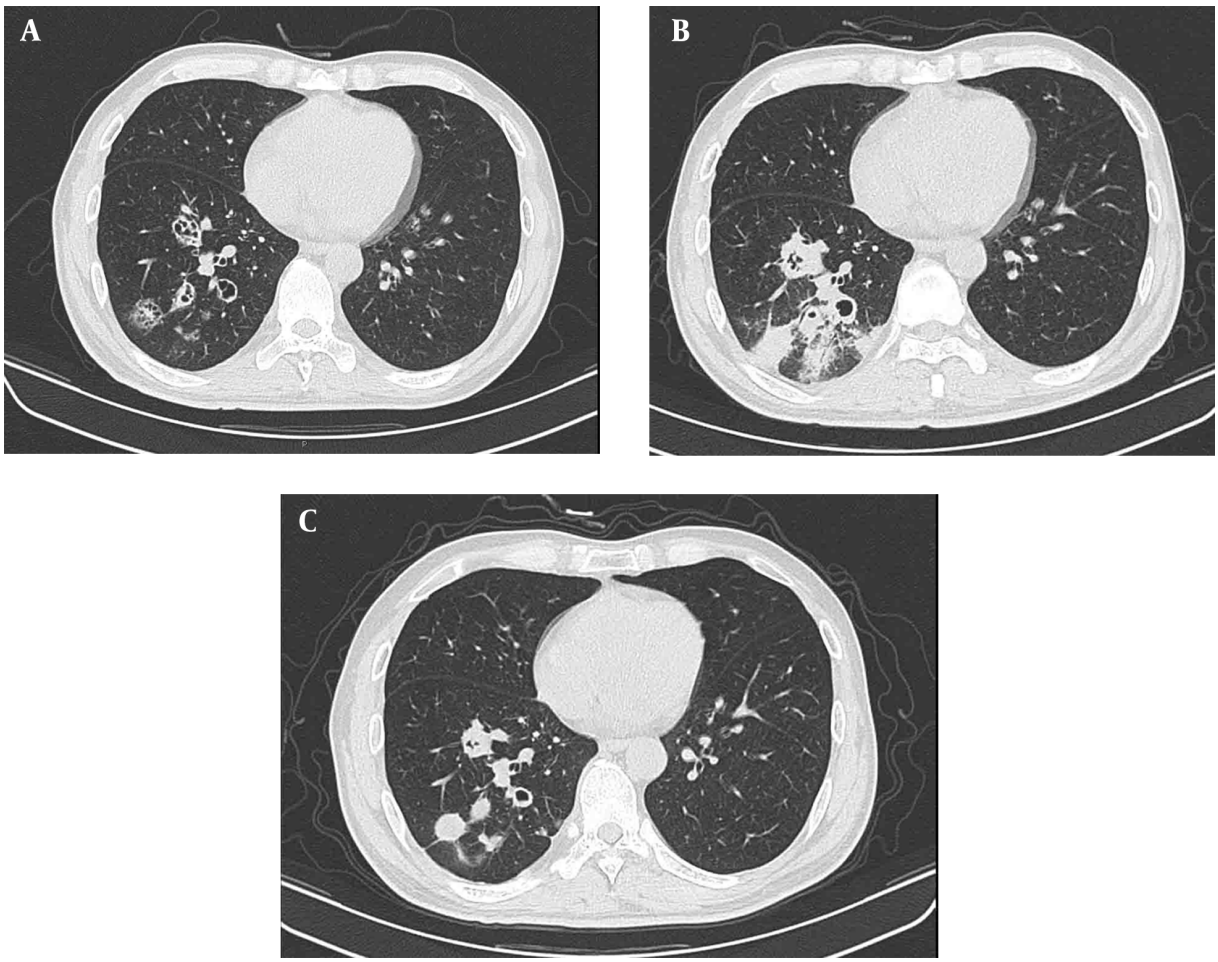

Figure 2. A-C, Pulmonary cryptococcosis (PC) in a 43-year-old man diagnosed with AIDS. CT scan (A) shows several cluster cavities in the right lower lobe, one of which is a cavity in wall (CW) lesion', while others are thin-walled cavities with a CD4 cell count of 12/μL. Pulmonary lesions progressed to pneumonic infiltrates with ill-defined margins (B) two weeks after highly active antiretroviral therapy (HAART), with a CD4 cell count of 30/μL. In a review CT scan (C) after five months, cavities and consolidation had become solid nodules with clear borders with the normal lung, and the CD4 cell count in peripheral blood increased to 158/μL.

systemic complications, especially cryptococcal meningitis which was detected in the majority of patients (38/62). All lesions were distributed in less than three lobes, including 29 (56.9%) patients with lower lobe involvement, 21 (41.2%) patients with upper lobe involvement, and 1 (1.9%) case of middle lobe involvement. Additionally, there were 14 patients with lymphadenopathy and six patients with pleural effusion.

4.2. Relationship Between Chest CT Findings and HIV Viral Load

The pulmonary abnormalities observed in the initial CT scans and the HIV viral load in the peripheral blood of patients with different types of lesion upon diagnosis are summarized in Table 2. Different types of cavity within nodules/masses (68.4%) were the most common radiological findings. The TNC, TKC, TC, and CW lesions accounted for 32.9%, 13.9%, 16.5%, and 5.1% of radiological cavitation findings, respectively. Solid nodules (27.9%) with well-defined margins or halo signs were the second most common finding. There were also 11 (13.9%) patients with solitary nodules, 7 (8.9%) patients with multiple nodules, and 4 (5.1%) patients with miliary nodules. Another lesion pattern was consolidation, detected in 3.8% of the patients.

The HIV viral load in peripheral blood was measured at the time of diagnosis before any antiretroviral therapy. There was no significant difference regarding the HIV viral load between different subgroups based on the lesion morphology (S vs. CA, P = 0.932; S vs. C, P = 0.588; and CA vs. C, P = 0.654). In the solid nodule group, the HIV viral load of patients with miliary nodules was significantly higher than

Table 1. Clinical and Radiological Characteristics of the Patients

Clinical characteristics	No. (%)
Gender	
Male	59 (95.16)
Female	3 (4.84)
Age (y), mean ± SD (range)	36.97 ± 11.91 (19 - 77)
Cell count (cells/μL)	P50; IQR (P25, P75)
CD4	23; (11, 42.5)
CD8	491; (269.5, 769)
CD4/CD8 ratio	0.05; (0.03, 0.09)
Symptoms	
Respiratory symptoms	14 (15.73)
Cough	8 (8.99)
Expectoration	6 (6.74)
Chest tightness	3 (3.37)
Dyspnea	2 (2.25)
Neurological symptoms	31 (34.83)
Headache	24 (26.97)
Dizziness	7 (7.87)
Mental disorders	1 (1.12)
Fever or fever combined with other symptoms	39 (43.82)
Other symptoms	5 (5.61)
Cryptococcosis	
Only pneumonia	24 (38.71)
Pneumonia + meningitis	38 (61.29)
Comorbidities	
PCP	14 (18.92)
CMV	12 (16.22)
TB	3 (4.05)
Syphilis	5 (6.76)
Malignant tumor (cervical cancer)	1 (1.35)
Lesion location	
One lobe	30 (48.4)
Two or more lobes	32 (51.6)
Lung involvement	
Right lung	31 (50.0)
Left lung	20 (32.3)
Bilateral	11 (17.7)

Abbreviations: SD, standard deviation; P50, 50%; IQR, interquartile range; CD4, CD4-positive T lymphocytes; CD8, CD8-positive T lymphocytes; PCP, Pneumocystis carinii pneumonia; CMV, Cytomegalovirus pneumonia; TB, tuberculosis.

that of patients with the other two types of nodules (MINs vs. SNs, P = 0.009; MINs vs. MNs, P = 0.024). In the cavitary group, the HIV viral load of patients with thick-walled cavity lesions was higher than that of patients with thin-walled cavity lesions, and the difference was statistically significant (P = 0.036).

4.3. Correlation Between CD4 Cell Count and Changes in the Lesion Morphology

After HAART, 81.5% of lesions (44 lesions in 40 patients) were classified in the improvement group. Nine nodules (16.7%) decreased, 7 (12.9%) cavity wall nodules became thinner, and 28 (51.9%) cavities became solid nodules. Ten lesions were classified in the progression group, including one enlarged nodule (1.9%), one solitary nodule that developed into multiple nodules (1.9%), two nodules transforming into a cavity (3.7%), three thickened cavity wall nodules (5.6%), and three cases of infiltration with ill-defined margins (6.5%). Forty HIV-infected patients with the median number of CD4 cell count is 23.88 ± 17.51/μL in peripheral blood upon diagnosis, which increased to 96.00 ± 71.55/μL in the 3 - 6-month follow-up after HAART.

Changes in the CD4 cell count during HAART were also recorded. The mean CD4 cell count increment was 70.6 ± 56/μL in the improvement group and 28.3 ± 19.9/μL in the progression group. There was a significant difference in the mean CD4 cell count increment between the improvement and progression groups (P = 0.001). The cut-off value for the CD4 cell count increment to differentiate the two outcomes (i.e., improvement and progression) was 44/μL, with an AUC of 0.851 (95% CI: 0.81 - 0.88) and sensitivity, specificity, and accuracy of 0.815, 0.714, and 0.764, respectively (Figure 3). Regarding agreement between the two radiologists, the ICC was in the range of 0.824 - 0.871.

5. Discussion

Only few studies on PC have focused on the correlation between CT findings and CD4 cell count or HIV viral load in immunocompromised patients, and most of these studies are case reports or have a small sample size (10, 11). On the other hand, the majority of studies with a larger sample size have concentrated on the clinical and imaging characteristics of Cryptococcus in different immune states (3, 12) or have simply compared the clinical and imaging features of immunocompetent and immunocompromised patients (13). In the present study, the chest CT manifestations of pathologically diagnosed PC were divided into three categories: Nodules, cavities, and consolidation. The CT features were also compared with the HIV viral load of patients at the time of examination, and changes in the

Table 2. Relationship Between Chest CT Findings and HIV Viral Load

Pulmonary lesions	No. (%)	HIV viral load (copies/mL)		P-value	
		P50	IQR (P25, P75)	Within groups [a]	Between groups [b]
Solid nodules				SN vs. MN 0.721; MN vs. MIN 0.024; SN vs. MIN 0.009	
Solitary nodules	11 (13.92)	2.43E+04	(3.25E+03 [c], 1.30E+05)		
Multiple nodules	7 (8.86)	6.78E+04	(1.75E+04, 2.50E+05)		
Miliary nodules	4 (5.06)	3.01E+05	(1.79E+05, 1.72E+06)		
Count	22 (27.85)	5.75E+04	(7.18E+03, 2.29E+05)		
Cavitation				TC vs. TNC 0.700; TC vs. TKC 0.122; TC vs. CW 0.862; TNC vs. TKC 0.036; TNC vs. CW 0.669; TKC vs. CW 0.356	S vs. CA 0.932; CA vs. C 0.654; C vs. S 0.588
Tiny cavity	13 (16.46)	2.44E+04	(1.15E+04, 1.36E+05)		
Thin-walled cavity	26 (32.91)	1.17E+05	(4.67E+04, 2.57E+05)		
Thick-walled cavity	11 (13.92)	1.27E+05	(8.52E+04, 3.74E+05)		
Cavity in wall	4 (5.06)	8.17E+04	(6.41E+04, 6.17E+05)		
Count	54 (68.35)	1.03E+05	(4.21E+04, 2.29E+05)		
Consolidation	3 (3.8)	2.43E+04	(5.24E+03, 6.10E+05)	-	

Abbreviations: HIV, human immunodeficiency virus; P50, 50%; IQR, interquartile range; S, solid nodules; CA, cavitation; C, consolidation; SN, solitary nodules; MN, multiple nodules; MIN, miliary nodules; TC, tiny cavity; TNC, thin-walled cavity; TKC, thick-walled cavity; CW, cavity in wall; CT, computed tomography.
[a] Between groups: Comparisons between three groups of S, C, and CA.
[b] Within groups: Comparisons between subgroups of patients in each main category of solid, cavitation, and consolidation.
[c] E+03: Scientific notation, representing E to the third power.

lung lesion morphology and CD4 cell count after HAART were analyzed to represent progression or improvement.

Currently, the World Health Organization (WHO) considers the CD4 cell count to be the gold standard for assessing the progression of major opportunistic infections and screening, prophylaxis, and treatment to decrease mortality in patients (14). However, according to the WHO in 2016, when patients are diagnosed with HIV, HAART should be initiated as soon as possible, regardless of the CD4 cell count (15). Meanwhile, detection of HIV load can better indicate an individual's response to treatment (16); therefore, we measured the HIV viral load to determine its correlation with lung lesions. The viral load decreased rapidly after the onset of HAART, although there was no significant change in the lung lesions. It was suggested that the CD4 cell count increment could reflect the progression or improvement of lung lesions.

The majority of previous studies have divided the CT manifestations of PC into two types: Focal nodular lesions and infiltrating lesions in HIV-negative patient, and solid nodule was the most common lesion type in the lungs (17). In this study, CT findings were classified into three categories of nodules, cavities, and consolidations, according to the number and morphology of nodules. This classification was mainly based on previous research, because with a weakened immune system, the proportion of cavitary lesions and invasive consolidation lesions increases (18). In the current study, the cavitary lesions accounted for 68.34% of all lesions; this rate is much higher than the rates reported in previous studies on HIV-negative patients. It should be noted that if nodules and cavitation are classified in the same category, observations may be deviated or inaccurate. Besides, cavitary and nodular lesions were further classified into different subtypes to further explore the relationship between different morphological lesions and immunodeficiency in the groups.

This study revealed that the HIV viral load of thick-walled cavitary and miliary nodules was higher than that of other nodule types; this difference is mainly attributed to pathological changes after PC inhalation in humans. PC is generally transmitted through the respiratory tract, and fungal spores deposit in the alveoli for colony growth (19). Since a gel-like capsule is wrapped around bacteria in the body, they have no direct contact with tissues, and tissue inflammation is relatively mild in immunocompromised patients; however, a more obvious inflammatory reaction appears when the capsule is lost. In brief, because the immune status of the hosts varies, the morphology of lesions in lungs infected by cryptococcal bacteria is diverse. When the immune status of the host body is good, crypto-

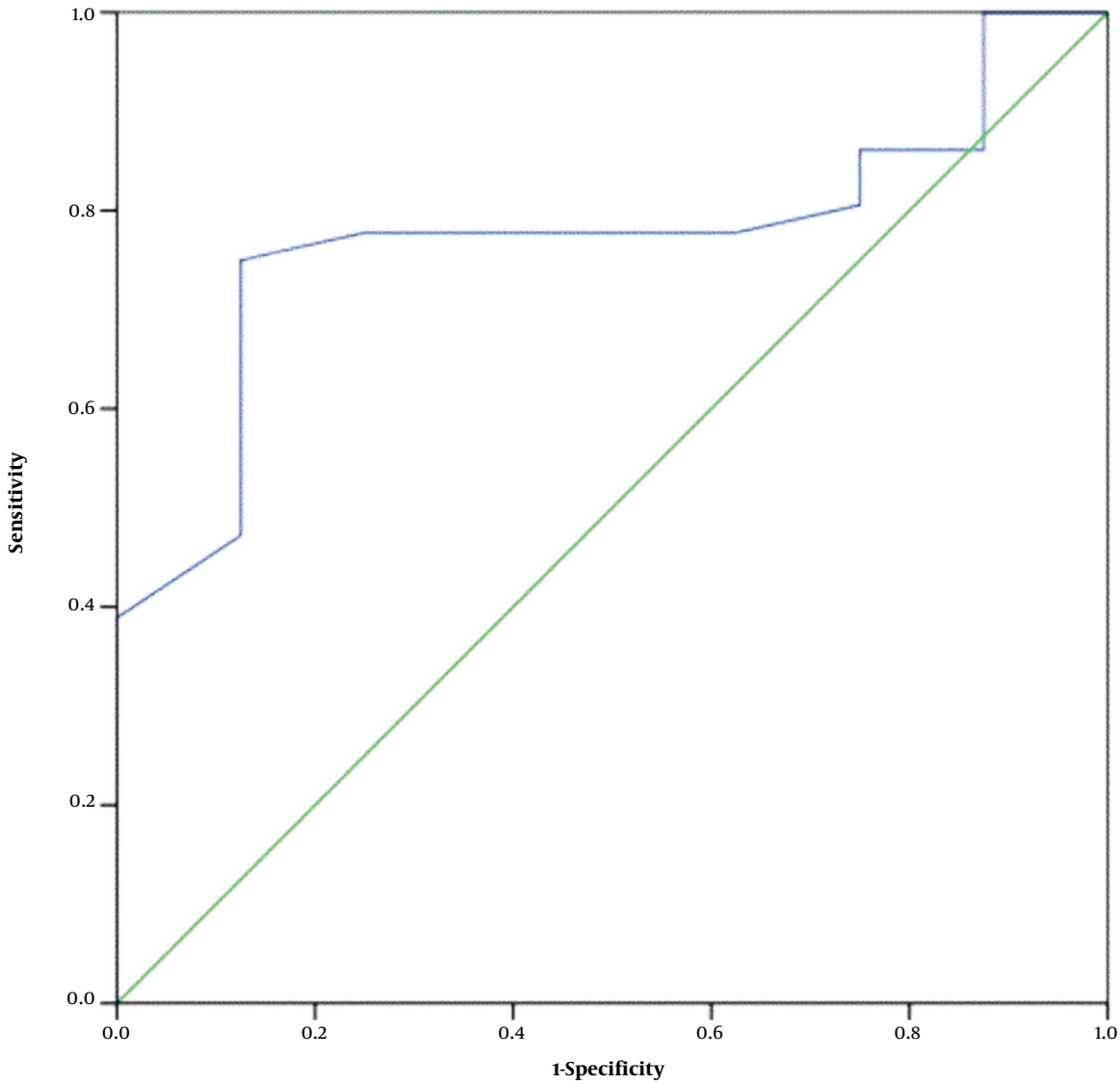

Figure 3. The receiver operating characteristic (ROC) curve for determining the cut-off value of CD4 cell count for differentiating two types of lesion morphology changes.

coccosis can induce delayed-type hypersensitivity after infecting the lungs, forming granulomatous nodules by the way to engulf the cryptococcal bacterium through lung macrophages and tissue cells, as well as fibroblasts and lymphocyte.

Masses can form when nodules fuse or granulomas continue to proliferate. Small focal areas of necrosis occur after the necrotic material is eliminated through the bronchus, and then, various types of cavitary lesions are formed. Consolidation pathologically includes a mixture of cryptococcal hyphae and mucus-denatured connective tissue (20). When the host immunity is impaired, the body's ability to form fibrotic granulomas decreases, leading to more or larger lung lesions, thickened cavity walls, and consolidation. In contrast, normal host immunity can promote the macrophage phagocytic immunity complex, activate CD8+ T cells to kill target cells, limit the scope of PC infection, and prevent large-scale lung dissemination, manifested in the lungs as reduced lesions, thinned cavity walls, and absorption or limitation of consolidation (21).

Based on the analysis of CD4 increment and the outcomes of pulmonary lesions after HAART, we concluded that a cut-off value of 44/μL for the CD4 increment could best predict the progression or improvement of pul-

monary lesions, with a diagnostic sensitivity of 81.5% and specificity of 71.4%. In this study, a follow-up of 3 - 6 months was performed after HAART to observe the CD4 cell count increment and lung lesion outcomes, mainly to reduce the possible influence of immune reconstitution inflammatory syndrome (IRIS) on the outcomes. IRIS is an immunomodulatory response after the onset of HIV reverse transcriptase therapy, reported in nearly 10% of anti-HIV therapies (22, 23). It is associated with various inflammatory factors and chemokines and can manifest as either deterioration of the original opportunistic infection or a new opportunistic infection in other sites, making the imaging process of the lungs complex and variable, as shown in Figure 2A-C.

Since IRIS is a self-limiting disease and also a response to excessive immune reconstitution during therapy, its emergence cannot be considered as disease progression (24). Currently, there are few studies on the occurrence of IRIS in PC. Some studies have reported that IRIS may appear in early stages (i.e., within a few days) after the onset of HAART. While after 6 - 12 months of treatment, the immune status of patients remains stable, the CD4 cell count does not significantly change, although the lung lesions continue to improve. Therefore, in this study, a follow-up of 3 - 6 months was performed to avoid the influence of the two mentioned factors on the results.

In conclusion, based on the present results, the HIV viral load and CD4 cell count in peripheral blood, which reflect the immune status of AIDS patients with PC, are related to the morphology and prognosis of pulmonary lesions, which can be helpful for clinical diagnosis and prognosis evaluation. However, the main limitation of this study was the small number of samples, and our conclusions need to be verified in a larger sample.

Acknowledgments

The authors would like to extend their sincere gratitude to American Journal Experts (AJE) for the English proofreading.

Footnotes

Authors' Contributions: ZZX and XRM designed the study; GCS was responsible for formal analysis; ZZX was responsible for methodology; XRM and CBD contributed to writing the original draft; and ZZX was responsible for writing-review and editing of the manuscript.

Conflict of Interests: This work was supported by Yv Miao Research Fund from Beijing Ditan Hospital, Capital Medical University (DTYM-202120). Employment: None. Personal financial interests: None. Stocks or shares in companies: None. Consultation fees: None. Patents: None. Personal or professional relations with organizations and individuals (parents and children, wife and husband, family relationships, etc.): None. Unpaid membership in a governmental or non-governmental organization: None. Are you one of the editorial board members or a reviewer of this journal? None.

Data Reproducibility: The datasets generated or analyzed in the current study are available from the corresponding author on reasonable request.

Ethical Approval: This retrospective study was approved by the Review Ethics Committee of Beijing Ditan Hospital, Capital Medical University under the ethical approval code, DTYM-2020 (approval code webpage: book.yunzhan365.com/mjvgs/vhhe/mobile/index.html).

Funding/Support: This work was supported by the Yv Miao Research Fund from Beijing Ditan Hospital, Capital Medical University, Beijing, China (DTYM-202120).

References

1. Qu W, Robinson M, Zhang FJ. Factors influencing the natural history of HIV-1 infection. *Chin Med J (Engl)*. 2008;**121**(24):2613–21. [PubMed ID: 19187605].
2. Jin X, Zhao SH, Gao J, Wang DJ, Wu J, Wu CC, et al. CT characteristics and pathological implications of early stage (T1N0M0) lung adenocarcinoma with pure ground-glass opacity. *Eur Radiol*. 2015;**25**(9):2532–40. [PubMed ID: 25725775]. https://doi.org/10.1007/s00330-015-3637-z.
3. He Q, Ding Y, Zhou W, Li H, Zhang M, Shi Y, et al. Clinical features of pulmonary cryptococcosis among patients with different levels of peripheral blood CD4(+) T lymphocyte counts. *BMC Infect Dis*. 2017;**17**(1):768. [PubMed ID: 29237413]. [PubMed Central ID: PMC5729485]. https://doi.org/10.1186/s12879-017-2865-z.
4. Hu Z, Xu C, Wei H, Zhong Y, Bo C, Chi Y, et al. Solitary cavitary pulmonary nodule may be a common CT finding in AIDS-associated pulmonary cryptococcosis. *Scand J Infect Dis*. 2013;**45**(5):378–89. [PubMed ID: 23244589]. https://doi.org/10.3109/00365548.2012.749422.
5. Xie LX, Chen YS, Liu SY, Shi YX. Pulmonary cryptococcosis: comparison of CT findings in immunocompetent and immunocompromised patients. *Acta Radiol*. 2015;**56**(4):447–53. [PubMed ID: 24757183]. https://doi.org/10.1177/0284185114529105.
6. Nadrous HF, Antonios VS, Terrell CL, Ryu JH. Pulmonary cryptococcosis in nonimmunocompromised patients. *Chest*. 2003;**124**(6):2143–7. [PubMed ID: 14665493]. https://doi.org/10.1016/s0012-3692(15)31671-8.
7. Zhu LP, Wu JQ, Xu B, Ou XT, Zhang QQ, Weng XH. Cryptococcal meningitis in non-HIV-infected patients in a Chinese tertiary care hospital, 1997-2007. *Med Mycol*. 2010;**48**(4):570–9. [PubMed ID: 20392150]. https://doi.org/10.3109/13693780903437876.
8. Watanabe Y, Kusumoto M, Yoshida A, Shiraishi K, Suzuki K, Watanabe SI, et al. Cavity Wall Thickness in Solitary Cavitary Lung Adenocarcinomas Is a Prognostic Indicator. *Ann Thorac Surg*. 2016;**102**(6):1863–71. [PubMed ID: 27663793]. https://doi.org/10.1016/j.athoracsur.2016.03.121.
9. Zhou F, Ma W, Li W, Ni H, Gao G, Chen X, et al. Thick-wall cavity predicts worse progression-free survival in lung adenocarcinoma treated with first-line EGFR-TKIs. *BMC Cancer*. 2018;**18**(1):1033. [PubMed ID: 30352571]. [PubMed Central ID: PMC6199793]. https://doi.org/10.1186/s12885-018-4938-9.

10. Qu J, Wang X, Liu Y, Lv X. Rapidly Progressive Pulmonary Cryptococcosis with Cavitation in an Immunocompetent Woman: A Case Report and Literature Review. *Southeast Asian J Trop Med Public Health*. 2017;**48**(1):179–83. [PubMed ID: 29644837].
11. Thornton CS, Larios O, Grossman J, Griener TP, Vaughan S. Pulmonary Cryptococcus infections as a manifestation of idiopathic CD4 lymphocytopenia: case report and literature review. *BMC Infect Dis*. 2019;**19**(1):862. [PubMed ID: 31623573]. [PubMed Central ID: PMC6798450]. https://doi.org/10.1186/s12879-019-4453-x.
12. Zhang J, Zhang D, Xue X, Yang L, Chen L, Pan L. Clinical analysis of 16 cases of pulmonary cryptococcosis in patients with normal immune function. *Ann Palliat Med*. 2020;**9**(3):1117–24. [PubMed ID: 32434369]. https://doi.org/10.21037/apm-20-897.
13. Qu J, Zhang X, Lu Y, Liu X, Lv X. Clinical analysis in immunocompetent and immunocompromised patients with pulmonary cryptococcosis in western China. *Sci Rep*. 2020;**10**(1):9387. [PubMed ID: 32523003]. [PubMed Central ID: PMC7287058]. https://doi.org/10.1038/s41598-020-66094-7.
14. Ehrenkranz PD, Baptiste SL, Bygrave H, Ellman T, Doi N, Grimsrud A, et al. The missed potential of CD4 and viral load testing to improve clinical outcomes for people living with HIV in lower-resource settings. *PLoS Med*. 2019;**16**(5). e1002820. [PubMed ID: 31141516]. [PubMed Central ID: PMC6541248]. https://doi.org/10.1371/journal.pmed.1002820.
15. World Health Organization. *Consolidated guidelines on the use of antiretroviral drugs for treating and preventing HIV infection: recommendations for a public health approach*. Geneva, Switzerland: World Health Organization; 2016.
16. Stover J, Bollinger L, Izazola JA, Loures L, DeLay P, Ghys PD, et al. What Is Required to End the AIDS Epidemic as a Public Health Threat by 2030? The Cost and Impact of the Fast-Track Approach. *PLoS One*. 2016;**11**(5). e0154893. [PubMed ID: 27159260]. [PubMed Central ID: PMC4861332]. https://doi.org/10.1371/journal.pone.0154893.
17. Yamakawa H, Yoshida M, Yabe M, Baba E, Okuda K, Fujimoto S, et al. Correlation between clinical characteristics and chest computed tomography findings of pulmonary cryptococcosis. *Pulm Med*. 2015;**2015**:703407. [PubMed ID: 25767722]. [PubMed Central ID: PMC4342071]. https://doi.org/10.1155/2015/703407.
18. Wang Y, Gu Y, Shen K, Cui X, Min R, Sun S, et al. Clinical features of cryptococcosis in patients with different immune statuses: a multicenter study in Jiangsu Province-China. *BMC Infect Dis*. 2021;**21**(1):1043. [PubMed ID: 34625036]. [PubMed Central ID: PMC8499499]. https://doi.org/10.1186/s12879-021-06752-x.
19. Hung MS, Tsai YH, Lee CH, Yang CT. Pulmonary cryptococcosis: Clinical, radiographical and serological markers of dissemination. *Respirology*. 2008;**13**(2):247–51. [PubMed ID: 18339023]. https://doi.org/10.1111/j.1440-1843.2007.01202.x.
20. Wang D, Wu C, Gao J, Zhao S, Ma X, Wei B, et al. Comparative study of primary pulmonary cryptococcosis with multiple nodules or masses by CT and pathology. *Exp Ther Med*. 2018;**16**(6):4437–44. [PubMed ID: 30542394]. [PubMed Central ID: PMC6257807]. https://doi.org/10.3892/etm.2018.6745.
21. Okubo Y, Tochigi N, Wakayama M, Shinozaki M, Nakayama H, Ishiwatari T, et al. How histopathology can contribute to an understanding of defense mechanisms against cryptococci. *Mediators Inflamm*. 2013;**2013**:465319. [PubMed ID: 24058271]. [PubMed Central ID: PMC3766597]. https://doi.org/10.1155/2013/465319.
22. Perfect JR, Dismukes WE, Dromer F, Goldman DL, Graybill JR, Hamill RJ, et al. Clinical practice guidelines for the management of cryptococcal disease: 2010 update by the infectious diseases society of america. *Clin Infect Dis*. 2010;**50**(3):291–322. [PubMed ID: 20047480]. [PubMed Central ID: PMC5826644]. https://doi.org/10.1086/649858.
23. Wong CS, Richards ES, Pei L, Sereti I. Immune reconstitution inflammatory syndrome in HIV infection: taking the bad with the good. *Oral Dis*. 2017;**23**(7):822–7. [PubMed ID: 27801977]. [PubMed Central ID: PMC5411339]. https://doi.org/10.1111/odi.12606.
24. Chang CC, Sheikh V, Sereti I, French MA. Immune reconstitution disorders in patients with HIV infection: from pathogenesis to prevention and treatment. *Curr HIV/AIDS Rep*. 2014;**11**(3):223–32. [PubMed ID: 24950732]. https://doi.org/10.1007/s11904-014-0213-0.